Removal of alpha-wave artefacts in MEG data by independent component analysis

T.H. Sander[1,2], A. Lueschow[2], G. Curio[2], and L. Trahms[1]

[1] *Physikalisch-Technische Bundesanstalt, 10587 Berlin,* [2] *Neurophysics Group, Universitätsklinikum Benjamin Franklin, 12200 Berlin, Germany*

1 Introduction

It is well known from electro-encephalographic (EEG) and magneto-encephalographic (MEG) recordings that the human brain generates spontaneous oscillatory signals at various frequencies. Probably the best known are the α waves with a typical frequency of 10 Hz, which are related to reduced vigilance or a state of low mental activity. These α waves can severely corrupt the stimulus triggered average in evoked response experiments.
Motivated by the observation of 10 Hz contamination in averaged Visually Evoked Fields (aVEF) obtained without inter-stimulus interval randomization, we performed an Indepedent Component Analysis (ICA) on raw unaveraged data. It was the aim to identify the source of the 10 Hz contamination and to remove it. The Temporal Difference source SEParation (TDSEP) algorithm [1, 2] was applied as it is very well suited for oscillatory data containing signals with distinct spectral features [3]. The identification of noise sources is generally an important topic as their efficient removal will improve the analysis of individual evoked epochs and their variability.
Other work [4] has studied the relation between α waves and motor responses using a different ICA algorithm.

2 Methods

2.1 Visually evoked fields

In normal subjects the MEG was recorded with a planar 49 channel gradiometer [5] centered over T6. Grey tone images of houses and faces were presented for 500 ms and masked for another 1.5 s leading to a total epoch length of 2.0 s. Using a block design either a face or a house was the attended target (press button) to study attention related effects. Here we focus on the separation of artefactual signal components.
The four field maps shown in Fig. 1 correspond to the most important features of an aVEF calculated from 90 non-consecutive epochs. Image presentation started at 0 ms and a first maximum is reached 160 ms later as shown in the first map. The data in Fig. 1 correspond to the case that the attention was focused on faces and a face was presented.

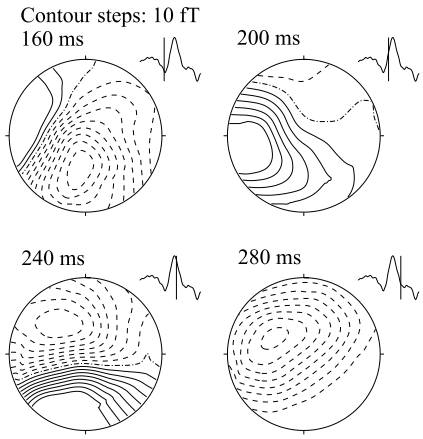

Figure 1: *Four field maps of a typical aVEF measured over T6. The image presentation started at 0 ms. The field pattern changes rapidly as the map sequence shows.*

In Fig. 2a) we show the superimposed time traces of the 49 MEG channels for the same aVEF as in Fig. 1. The main activity starts at 160 ms. Weaker activity is already present at 130 ms and even at -100 ms, before image presentation at 0 ms. This activity cannot be related to the image presentation without violating causality. Spectral analysis of the aVEF reveals that the signal before image presentation is mainly an oscillation with a frequency of 10 Hz. A spectral analysis of the raw unaveraged data gives a strong 10 Hz peak, which increases in strength as the experiment proceeds. The aVEF shown in Fig. 2a) is an average from the last block of an experiment containing in total three blocks each of 20 minutes duration. We have chosen the last block as the 10 Hz oscillations are strongest in this block and therefore the need to remove the contamination is most urgent. Certain subjects showed strong 10 Hz oscillations throughout the experiment.

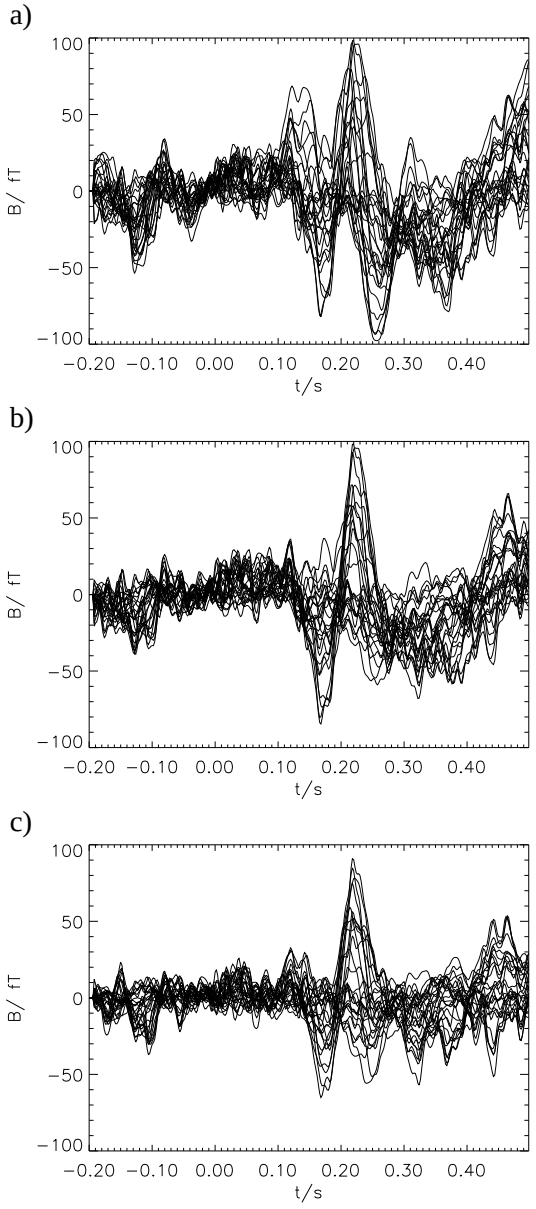

Figure 2: *a) Butterfly plot of the aVEF shown in Fig. 1. Even before image presentation at 0 s large oscillations with a periodicity of 100 ms are visible. b) From the data in a) the component ICA1 of Fig. 3 has been removed. c) The components ICA1, 3, 5, 10 and 11 (not shown) have been removed from the data in a).*

2.2 Temporal Difference source SEParation

In MEG recordings an unknown number of brain and external (noise) sources is present. It is difficult to model this in full generality and commonly a simple linear model is used. It is assumed that the recorded data are a linear superposition of n sources $s_i(t)$ with a constant source pattern a_{ji}, which are measured in a sensor system having m channels yielding $x_j(t)$ time traces. To describe this in an invertible linear equation $m \geq n$ is required and the model can be written as

$$\underline{\mathrm{x}}(t) = \underline{\mathbb{A}}\underline{\mathrm{s}}(t). \tag{1}$$

The sources $s_i(t)$ and their patterns are generally unknown. A demixing matrix $\underline{\mathbb{W}}$ is searched for, which fulfills

$$\underline{\mathrm{u}}(t) = \underline{\mathbb{W}}\underline{\mathrm{x}}(t), \tag{2}$$

where the $u_i(t)$ are identical to the $s_i(t)$ disregarding an indeterminancy in scale and ordering. This needs to be resolved in the sense, that the sources can be ordered by their strength to discriminate between strong and weak sources. This is achieved by normalizing the vectors of $\underline{\mathbb{W}}$ and then calculating the Euclidean norm (L2-norm) of the resulting $u_i(t)$.
ICA is a method to estimate the demixing operator $\underline{\mathbb{W}}$ using the assumption of statistical independence between sources. This independence is equivalent to a probability density function factorising into the individual densities as shown:

$$p(s_1, ..., s_n) = \prod_{i=1}^{n} p_i(s_i). \tag{3}$$

The factorization means, that the covariance matrix and time-delayed covariance matrices are diagonal with respect to the $s_i(t)$. The TDSEP [1, 2] algorithm utilizes this as it tries to simultaneously diagonalize several time-delayed covariance matrices to estimate the demixing matrix $\underline{\mathbb{W}}$.
For interpretation and assessment the blindly calculated $u_i(t)$ and their patterns $\underline{\mathbb{W}}^{-1}$ can be compared afterwards to secondary information. A simple example is the heartbeat. Together with the MEG a single electrocardiogram (ECG) channel can be recorded and this time series can be compared to each of the $u_i(t)$.

3 Results

3.1 TDSEP applied to raw data

The TDSEP algorithm was applied to a dataset of 80 s length corresponding to 40000 datapoints for each of the 49 sensor channels. Twenty time delayed covariance matrices offset by 2 ms were used. This dataset is 10 % of the full data set. The results do not differ considerably using the full set. By using smaller data subsets it is possible to compare the result from

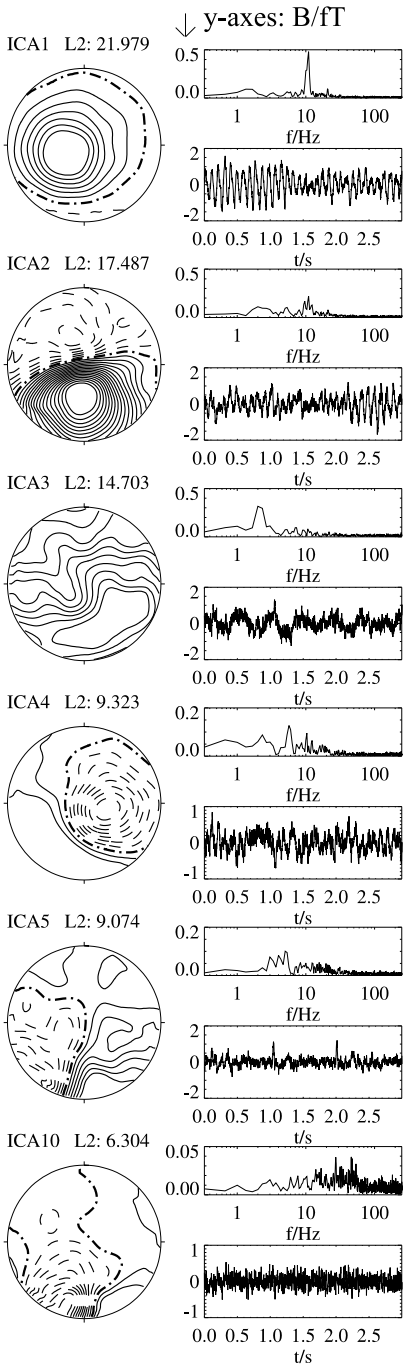

Figure 3: *ICA decomposition of multichannel raw MEG data using TDSEP. Component ICA1 has a peak at 10 Hz in its spectrum and is attributed to α waves, ICA2 has a broad spectrum and its map is similar to the map at 240 ms in Fig. 1. ICA4 cannot be associated immediately to a known source. ICA3 and 5 are attributed to the heartbeat, and finally ICA10 is possibly caused by muscular activity in the neck.*

different regions in the dataset and to exclude regions of strong external noise or rest periods of the subject, which are severely contaminated by eye blinks.

The result of the decomposition using TDSEP is shown in Fig. 3. For each component three types of visualization are given, the field map (i.e. the columns of $\underline{\mathbf{W}}^{-1}$), the time series (i.e. $u_i(t)$), and the spectrum of the time series. The time series is only a short excerpt from the 80 s used in the calculation. The components are ordered by the value of their L2-norm given as 'L2' in the figure.

The first component *ICA1* shows amplitude modulated 10 Hz oscillations. In *ICA2* the lower frequency components are nearly as strong as the 10 Hz oscillations. The field maps of *ICA1* and *2* resemble the aVEFs in Fig. 1 at 280 and 240 ms. The smooth and almost monopolar field map of *ICA4* implies that it is related to cortical activity, although it cannot be identified with parts of the aVEF. Component *ICA4* is either due to a failure of the ICA model (e.g. $n > m$, statistical dependence between the $s_i(t)$, etc.) or due to the presence of a real physiological signal not visible in the average and not known from secondary information.

Component *ICA 5* is related to the QRS-complex of the heartbeat as its time series is similar to a simultaneously recorded ECG. The raw data averaged with respect to the R-peak showed for certain times a field map very similar to *ICA 5* and was for other times similar to *ICA 3*. The field maps of *ICA 3* and *5* show gradients typical for a remote source as it is the heart. The distortions in the gradient are due to the detector geometry relevant for remote sources. Component *ICA10* has a field maximum at the lower edge of the sensor. This was the position of the neck in the measurement and muscular tension seems to be a possible origin. This is supported by its spectrum having a broad maximum at 40 Hz. A component due to 50 Hz power line noise looks very different (not shown).

3.2 Noise supression by demixing

As the TDSEP decomposition in Fig. 3 has resulted in two components containing 10 Hz oscillations it appeared promising to demix the measured signal and recombine it omitting one or several of the components. This is done mathematically by setting the corresponding column(s) in $\underline{\mathbf{W}}^{-1}$ to zero.

Firstly the component with the strongest 10 Hz signal is omitted (*ICA1*), and the result is shown in Fig. 2b). The oscillations before image presentation at 0 ms and between 300 and 400 ms are clearly reduced as is positive activity at 130 ms and a negative peak at

255 ms. The physiologically most interesting early activity between 160 and 240 ms remains essentially unchanged. The reduction of the 10 Hz oscillations in the aVEF due to omitting component *ICA1* implies that the 10 Hz oscillations present in the raw data appear in the average.
Omitting *ICA2* the aVEF is strongly modified in the region between 160 and 240 ms indicating that *ICA2* is related to the early aVEF. The dual role of *ICA1* and *2* in describing parts of the aVEF together with oscillatory activity is either due to an incomplete demixing or it is of physiological origin, i.e. VEF and the 10 Hz oscillations originate from the same cortical location. In Fig. 2c) the components *ICA1*, *3*, *5*, *10* and *11* (50 Hz power line noise, not shown) have been omitted. The signal to noise ratio before the physiologically expected aVEF onset at 100 ms seems further improved implying artefacts in the aVEF due to the heartbeat or power line noise. This has to be assessed yet quantitatively.
The two TDSEP components containing 10 Hz oscillations are the strongest signals of the raw data section used in Fig. 3 as they have the largest values of L2. Therefore it should be possible to observe them in bandpass filtered raw data. Using a filter of width 5 - 15 Hz field maps similar to *ICA1* and *2* can be seen at the same times as in Fig. 3. Taken all facts together we identify the 10 Hz oscillations with α waves. This is further supported by the amplitude modulation occurring in the time series of *ICA1* and *2*.
The amplitude of the α waves in the filtered data is up to 1 pT. The 10 Hz oscillations before stimulus onset peak at 50 fT in Fig 2a). Assuming the α waves to be uncorrelated to the stimulus they should be reduced in the aVEF by a factor of $90^{1/2} \approx 9.5$. Given the intermittent nature of α waves this agrees well with observation.
Note that simple bandpass filtering cannot yield the same result as the TDSEP decomposition. The filter result is due to the combined pass band spectral density of all signals, i.e. α waves, heartbeat, VEF and other sources.

4 Conclusions

Motivated by a 10 Hz contamination in an aVEF we performed an TDSEP-ICA on MEG raw data. Significant components can be attributed to α waves, the heartbeat, muscular tension in the neck and the VEF itself. Omitting the strongest component attributed to α waves the aVEF is considerably improved. Clearly the effectiveness of the method depends on the orientation of the dominant α field map compared to physiologically interesting parts of the aVEF, which was very favourable here and for other subjects. Only in the case of a subject reporting fatigue after the experiment it was not possible to improve the aVEF. Future work will focus on using TDSEP to isolate components solely attributable to the VEF.

Acknowledgements

Stimulating discussions with G. Wübbeler, G. Nolte, A. Ziehe, and K.-R. Müller and the usage of their software packages is gratefully acknowledged. This work is supported by the DFG grant number Ma 1782/1-4.

References

[1] A. Ziehe and K.-R. Müller, "TDSEP - an efficient algorithm for blind separation using time structure", in *Proc. Int. Conf. on Artificial Neural Networks (ICANN'98)*, L. Niklasson, M. Bóden, and T. Ziemke Eds., Springer Verlag, 1998, pp. 675–680.

[2] A. Belouchrani, K. Abed-Meraim, J.-F. Cardoso, and E. Moulines, "A blind source separation technique using second-order statistics", *IEEE Trans. Sign. Proc.* **45**(2), 434–444, 1997.

[3] A. Ziehe, G. Nolte, G. Curio, and K.-R. Müller, "OFI:Optimal filtering algorithms for source separation", in *Proc. of the 2nd Intern. Workshop on Independent Component Analysis and Blind Signal Separation*, P. Pajunen, and J. Karhunen Eds., Helsinki, 2000, pp. 127–132.

[4] T.-P. Jung, S. Makeig, M. Westerfield, J. Townsend, E. Courchesne, and T.J. Sejnowski, "Analyzing and visualizing single-trial event-related potentials", in *Advances in Neural Information Processing Systems 11*, MIT press, 1999, pp. 118–124.

[5] D. Drung, "The PTB 83-SQUID-system for biomagnetic applications in a clinic" ,*IEEE Trans. Appl. Supercond.* **5**, 2112–2117, 1995.